Crystal Structures of a Psychrophilic Metalloprotease Reveal New Insights into Catalysis by Cold-Adapted Proteases

Nushin Aghajari,[1]* Filip Van Petegem,[2] Vincent Villeret,[2] Jean-Pierre Chessa,[3] Charles Gerday,[3] Richard Haser,[1] and Jozef Van Beeumen[2]*

[1]*Institut de Biologie et Chimie des Protéines, UMR 5086, Laboratoire de Bio-Cristallographie, CNRS et Université Claude Bernard Lyon I, Lyon, France*

[2]*Laboratorium voor Eiwitbiochemie en Eiwitengineering, Universiteit Gent, Gent, Belgium*

[3]*Laboratoire de Biochimie, Institut de Chimie B6, Université de Liège, Liège, Belgium*

ABSTRACT **Enzymes from psychrophilic organisms differ from their mesophilic counterparts in having a lower thermostability and a higher specific activity at low and moderate temperatures. It is in general accepted that psychrophilic enzymes are more flexible to allow easy accommodation and transformation of the substrates at low energy costs. Here, we report the structures of two crystal forms of the alkaline protease from an Antarctic *Pseudomonas* species (PAP), solved to 2.1- and 1.96-Å resolution, respectively. Comparative studies of PAP structures with mesophilic counterparts show that the overall structures are similar but that the conformation of the substrate-free active site in PAP resembles that of the substrate-bound region of the mesophilic homolog, with both an active-site tyrosine and a substrate-binding loop displaying a conformation as in the substrate-bound form of the mesophilic proteases. Further, a region in the catalytic domain of PAP undergoes a conformational change with a loop movement as large as 13 Å, induced by the binding of an extra calcium ion. Finally, the active site is more accessible due to deletions occurring in surrounding loop regions. Proteins 2003;50:636–647.** © 2003 Wiley-Liss, Inc.

Key words: extremophile; psychrophile; crystallography; adaptation; temperature

INTRODUCTION

Numerous bacteria live at temperatures close to 0°C. To survive and grow at such conditions, these organisms have evolved several adaptations of their cellular components, especially of their enzymes.[1–4] The cold-adapted proteins have an increased turnover number and physiological efficiency (k_{cat}/K_m) at low and moderate temperatures. The structures of four psychrophilic enzymes have recently been determined by crystallography,[5–9] while in the past homology modelling was more commonly used.[10–14] Comparison with their mesophilic counterparts has allowed us to pinpoint to some extent the molecular basis of cold adaptation. In general, it is accepted that cold-adapted proteins are more flexible, with a reduced number of stabilizing interactions.[1–4] Loops are often longer and more hydrophilic,[4] the proline and arginine contents can be lower, and there is often an increased number of glycine residues. The surface of the molecular structures can display a lower content of charged residues and a higher proportion of hydrophobic side-chains.[5,14] The number of known psychrophilic enzyme structures is still small, however, and more studies are required to improve the understanding of the structural basis of cold adaptation of these enzymes. Moreover, for comparative studies it is critical to have the structures of mesophilic (and, if available, thermophilic and hyperthermophilic) counterparts to account for changes that may be linked to psychrophily.

Here, we report the structures of a psychrophilic alkaline protease (PAP) from *Pseudomonas* TAC II 18 sp. in two different crystal forms. The organism was isolated from Antarctica and the protein characterized.[15] The 463-residue enzyme is 3 times more active at 20°C than a mesophilic counterpart from *Pseudomonas aeruginosa*. At 45°C, the psychrophilic enzyme is rapidly inactivated and the protein is sensitive to small concentrations (2 mM) of ethylenediaminetetraacetic acid (EDTA). At present, two mesophilic homologs with known tertiary structure have been characterized. One of them, the alkaline protease from *P. aeruginosa* (AP, 470 residues) shows 66% sequence identity with PAP and its structure was determined with and without a tetrapeptide in the active site.[16,17] Another metalloprotease, serralysin, also known as Serratia pro-

Grant sponsor: Fund for Scientific Research-Flanders; Grant number: G.0068.96; Grant sponsor: Bijzonder Onderzoeksfonds (University of Ghent); Grant number: GOA 12050198; Grant sponsor: E.U.; Grant numbers: BI04-CT96-0051 and CT97-0131; Grant sponsor: Centre National de la Recherche Scientifique; Grant sponsor: Fonds National de la Recherche Scientifique; Grant numbers: 2.4523.97 and 2.4515.00; Grant sponsor: Région Wallonne; Grant number: 9613492.

Both Nushin Aghajari and Filip Van Petegem contributed equally to this work.

*Correspondence to: Jozef Van Beeumen, Laboratorium voor Eiwitbiochemie en Eiwitengineering, Universiteit Gent, B-9000 Gent, Belgium. E-mail: jozef.vanbeeumen@rug.ac.be or Nushin Aghajari, Institut de Biologie et Chimie des Protéines, UMR 5086, Laboratoire de Bio-Cristallographie, CNRS et Université Claude Bernard Lyon I, F-69367 Lyon, Cedex 07, France. E-mail: n.aghajari@ibcp.fr

Received 20 November 2001; Accepted 1 August 2002

TABLE I. Crystallographic Data for the Two Crystal Forms of PAP

	Crystal	
	Form 1	Form 2
Crystallization condition	5–10% PEG 6000, 1 mM $CaCl_2$, 100 mM Tris-HCl at pH 8; protein concentration 20 mg/mL	1.6 M $(NH_4)_2SO_4$, 0.1 M Hepes buffer at pH 7.0; protein concentration of 15 mg/mL
Crystal growth temperature (°C)	4	19
Data collection temperature (°C)	21	15
Space group	$P2_12_12_1$	R3
Unit cell parameters	a = 54.00 Å, b = 57.55 Å, c = 161.81 Å, α = β = γ = 90°	$a = b$ = 186.01 Å, c = 37.97 Å, α = β = 90°, γ = 120°
No. molecules (a.u.)	1	1
Matthews Coefficient (Å^3/Da)	2.580	2.549
Refinement		
Resolution (Å)	15-2.1	46.13-1.96
R/R_{free}	16.4/22.1	15.6/18.7
No. protein atoms	3403	3481
No. water molecules	284	355
No. metal ions	9	8
No. sulphate ions	/	1
Average B-factor (Å^2)		
Main-chain	29.27	17.69
Side-chain	31.38	18.73
Water molecules	42.08	30.07
Metal ions	27.14	17.77
RMSD bond lengths (Å)	0.017	0.005
RMSD bond angles (°)	3.1	1.159
Ramachandran	93.0	89.3
% residues in most favored parts		

tease from *Serratia marcescens* (SMP, 471 residues), displays 55 % identity with the psychrophilic protease. Both the native structure of SMP and two of its complexes with different inhibitors have been determined.[18,19] The 3D structure of a second Serratia protease, from *Serratia* sp.E-15, is also known.[20] The mesophilic homologs are folded in two domains, with the catalytic N-terminal domain consisting of four helices and a mixed five-stranded β-sheet. The C-terminal domain, which may play a role in folding of the molecule after transmembrane translocation [16], forms an extended β-roll with 20 successive β-strands wound in a right-handed spiral. The structures of PAP were subjected to detailed comparative studies with those of the mesophilic AP and SMP proteins, and the relative flexibility of the psychrophilic and mesophilic enzymes was also studied by fluorescence quenching.

MATERIALS AND METHODS

Fluorescence Quenching

Fluorescence quenching experiments[21,22] were performed in the temperature range of 5–35°C for 30 min to avoid any denaturation of the protein. Concentrations of acrylamide ranged from 0–120 mM. A standard concentration of 10 μM enzyme was used in a buffer containing 20 mM Tris, pH 8, 1 mM $CaCl_2$. The protein solution was excitated at 280 nm and the fluorescence emitted at 337 nm was measured using a Perkin-Elmer LS50 fluorimeter with a thermostabilized quartz cell. The quenching values were corrected for the absorbance of acrylamide, according to $F_c = F_m\ 10^{-(\varepsilon Q)/2}$, where F_c and F_m are the corrected and measured fluorescence, respectively, ε the molar extinction coefficient, and Q the molar concentration of the quenching acrylamide. A graph of F_0/F_c as a function of the temperature allowed the determination of the Stern–Volmer constant K_D: $F_0/F_c = 1 + K_D\ (Q)$, where F_0 is the initial fluorescence.

Crystallization, Data Collection, and Molecular Replacement

Crystallization, data collection, and molecular replacement were described previously[23,24] and are partly summarized in Table I. For both crystal forms of PAP, the known structure of the *P. aeruginosa* alkaline protease[16] served as the model in a molecular replacement search performed with the program AMoRe.[25] As the primary structure was unknown, initial models were polyalanine chains.

Refinement and Building of the Model

Both crystal forms were obtained prior to the cloning of the alkaline protease gene, so refinement had to await the sequence before completion. Relevant statistics are given in Table I.

Form 1: The alanines in the initial model of form 1 were replaced by the appropriate residues when the sequence became available. The structure was refined with a maximum likelihood-based refine-

ment strategy employing the program REFMAC,[26] followed by manual fitting into SIGMAA-weighted[27] electron density maps with TURBO-FRODO.[28] A 2-Gaussian bulk solvent correction was applied. After calculation of an omit map, both the side- and main-chain of Tyr209 were positioned and refined in a double conformation, and occupancies for both conformations were set to 0.5. Two residues for which no electron density was visible for the side-chains were refined as glycines (Arg111 and Asn126). Due to poor or missing electron densities, residues1–2 and 184–188 were not inserted in the electron density map (neither the main-chain nor the side-chain). Stretches for which the density clearly deviated from the main-chain in the homologous model were first left out and repositioned after calculation of an omit map.

Form 2: Replacement of alanines in the initial polyalanine model with the actual amino acid residues was performed whenever it was possible to identify the side-chain in the electron density maps. The presence of all Ca^{2+} and Zn^{2+} ions was confirmed with an anomalous difference Fourier map calculated using the program CNS,[29] where F_{calc} comes from a refined model in which metal ions have been omitted. Refinement of the structure was performed using the program CNS and applying an overall anisotropic temperature factor correction algorithm, followed by manual fitting as described above. Due to poor or missing electron densities, as for form 1, residues 1–2, 112, and 184–187 were not inserted in the electron density map. Side-chain residues for Arg111 and Gln429 were refined as glycines and, as judged from the electron density, residue 22 is an Asp rather than a Glu predicted by sequence analysis; it has been refined as such. Double conformations were found for residues Ser15, Val55, Thr61, Gln80, Leu84, Ser138, Gln152, Leu242, Thr288, Ser306, Ser435, Leu436, and Val456.

Structure Analysis

Ramachandran plots for the final models were calculated with PROCHECK,[30] showing that all residues were in allowed regions. Multiple sequence alignment was performed with ClustalW.[31] The C_α atoms from matching residues in the alignment were superposed with LSQKAB.[26] Secondary structure elements were calculated with DSSP[32] and hydrogen bonds and salt bridges with HBPLUS[33] and ACT.[26] Accessible surfaces were determined with GRASP[34] and ACCESS.[26]

Accession Numbers

The two psychrophilic structures have been deposited in the RCSB Protein Data Bank under the entry codes 1H71 (form 1) and 1G9K (form 2) and will be accessible upon publication.

RESULTS AND DISCUSSION

Fluorescence Quenching

Local unfolding, resulting from the disruption of a few weak interactions so that usually buried sites become transiently exposed to the solvent, is a function of temperature and leads to complete unfolding of the protein when temperatures are sufficiently high. If cold-adapted enzymes display a high intrinsic flexibility, one can expect that the level of local unfolding, at a given temperature, should be higher than in the case of the corresponding mesophilic enzyme. A possible way of following the process is to measure the quenching effect of acrylamide on the intrinsic tryptophan fluorescence of the protein, the quenching phenomenon being proportional to the number of Trp residues and to their accessibilities. We performed such measurements for PAP and AP at different temperatures and different concentrations of acrylamide. The psychrophilic and mesophilic enzymes have, respectively, six and seven Trp residues. Six of the latter are at exactly the same position in both polypeptide chains, and the additional Trp in the mesophilic enzyme is located at the surface of the protein. Due to this difference, the absolute values of the Stern–Volmer constants K_D are expected to be higher for the mesophilic than the psychrophilic enzyme, at any given temperature. Changes in these values as a function of temperature are expected to depend on the way in which the accessibilities of the different tryptophan residues will vary. The graphical representation of K_D versus temperature (not shown), however, demonstrates that between 5 and 35°C, and at a constant acrylamide concentration of 0.1 M, the increase of K_D is higher for the psychrophilic enzyme ($\Delta K_D = 9$) than for the mesophilic enzyme ($\Delta K_D = 6$). To compensate for the additional Trp residue in AP, we also plotted the differences between the quenching effects obtained at 35 and 5°C as a function of acrylamide concentration (Fig. 1). One can observe a steeper change for the psychrophilic protein, indicating a greater increase in accessibility of the Trp residues in PAP, which may indicate a higher overall flexibility.

Overall Structure

The PAP molecule consists of a single chain of 463 amino acid residues, with one Zn^{2+} ion and 8 (form 1) or 7 (form 2) Ca^{2+} ions. Its tertiary structure is comparable to those of the available homologues AP and SMP, with the N-terminal domain comprising residues 20–247 and the C-terminal domain comprising residues 248–463 [Fig. 2(a)]. Residues 1–2 are not present in either one of the structures, nor are residues 184–188.

The superposition of the 3D structure of PAP with the two available mesophilic homologous structures [Fig. 2(b)], using all the C_α atoms of AP that are not part of an insertion or deletion in the sequence alignment (Fig. 3) and that are present in all structures, gives a root-mean-square deviation (RMSD) of 2.3 Å (form 1) or 2.5 Å (form 2). For SMP, the same superposition can be done with a 2.8-Å (form 1) or 2.9-Å (form 2) RMSD. The two 3D structures of PAP are similar as they superpose with an RMSD deviation of 0.83 Å for all aligned C_α atoms despite different

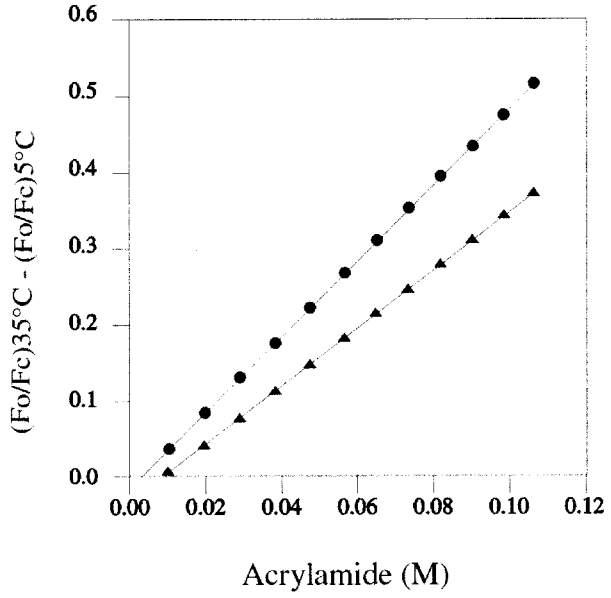

Fig. 1. Differences in quenching effects obtained at 35 and 5°C as a function of acrylamide concentration. Circles, psychrophilic enzyme; triangles, mesophilic enzyme; F_0, initial fluorescence; F_c, corrected fluorescence, taking the absorbance of acrylamide into account. At all concentrations of acrylamide , a bigger difference in quenching is visible for PAP than for AP. The curve is also steeper for PAP than for AP.

crystallization conditions and marked differences in crystal packing.

Catalytic Domain and Active Site

PAP is one of several metalloproteases for which a zinc ion is essential for the catalytic activity. These metalloproteases form the superfamily of "metzincins" comprising astacins, matrix metalloproteinases (collagenases), snake venom proteinases, and serralysins.[35] A feature that characterizes the metzincins is the sequence motif HEXXHXXGXXHZ (residues 169–180 in PAP), where the histidine residues are ligands to the Zn^{2+} ion and Z is characteristic for the different subfamilies. Further, a conserved methionine residue that is likewise characteristic of the metzincin superfamily is also present in PAP (Met207).

In the active site, the Zn^{2+} ion is coordinated in a trigonal–bipyramidal geometry to four, or five, ligands depending on the position of the Tyr209 [Fig. 4(a)]. The Zn^{2+} , when pentacoordinated, is bound to the side-chains of three His residues, Tyr209, and a water molecule. Imidazole nitrogens (NE) of His169 and His179, and the oxygen of the water molecule, are at the base of the bipyramid. The hydroxyl group of Tyr209 (in crystal form 1) and the imidazole nitrogen of His173 lie perpendicular to this triangle. The water molecule is also bound to the side-chain of Glu170, which is thought to be important in activating the water molecule during catalysis.[16] This zinc site is similar to those seen in AP and SMP, as well as to that observed in astacin, a zinc endopeptidase from the European freshwater crayfish.[35]

The electron density associated with Tyr209 in crystal form 1 is consistent with a double conformation of its side-chain. The main-chain is discretely disordered. In AP, it was shown that the corresponding residue (Tyr216) is displaced when the enzyme binds a peptide substrate.[17] In free AP, the hydroxyl group of this tyrosine serves as the fifth ligand for the Zn^{2+} ion whereas, upon substrate binding, the tyrosine hydrogen bonds to the main-chain of the bound peptide. This has been reported for SMP as well.[19] When superposed with the structures of the substrate-bound forms of AP or SMP, it can be seen that one of the two conformations of Tyr209 in crystal form 1 of PAP corresponds to that of the displaced residue in substrate-bound AP [Fig. 4(b)] and that it cannot coordinate the Zn^{2+} ion. The Tyr209 OH groups in the two conformations found in form 1 are separated by a distance of 2.8 Å compared to a displacement of 2.9Å of the corresponding group in AP when substrate binds. In crystal form 2, the electron density map corresponding to this residue is consistent with only one conformation of the active site tyrosine, corresponding also to the substrate-bound form of AP. In this form, the tyrosine hydroxyl group is at a distance of 2.3 Å from the zinc-coordinated conformation in form 1. Four different rotamers exist for tyrosine residues.[36] The $m - 30°$ rotamer is observed for the Tyr ligating the Zn ion in form 1, as for the Tyr in form 2 crystals, whereas the second conformation of Tyr in form 1 does not correspond to any common rotamer. The relative B-factors (see later) for Tyr209 lie in between those found in AP and SMP, with values of 105% (form 1), 113% (form 2), 98% (AP), and 144% (SMP).

In the ligand-bound structure of AP, the carboxyl group of the C-terminal residue of the tetrapeptide serves as a fourth and fifth ligand for the Zn^{2+} ion, replacing a water molecule and the tyrosine side-chain ligand in the free enzyme.[17] One can expect that the mechanism of binding and catalysis in PAP is analogous, and the loss of the Tyr–Zn^{2+} coordination may reflect a weaker Zn^{2+}—Tyr—OH bond. Therefore, the inherent flexibility of the Tyr209 side-chain in the psychrophilic protease might facilitate the coordination of the substrate to the Zn^{2+} site.

Four loops surround the active-site region. The structural results for AP suggested that two "flaps," corresponding to residues 126–129 and 182–189 in PAP, play a role in restricting the access to the substrate binding cleft, and thus in controlling the substrate specificity. As concerns the first flap, two different conformations are found when comparing the two PAP crystal forms, with a displacement of ≈6 Å for Gly127. This may be due to differences in crystal contacts between the two forms. In form 1, the loop is close to a solvent channel, whereas in form 2 it packs against a neighboring molecule. Compared to SMP, there is a six-residue deletion in this loop, which results in a higher accessibility to the active site in PAP. In AP, however, this loop has the same length as in PAP.

The second flap in AP (182–189, PAP numbering) has high B-factors and was shown to be displaced upon binding a peptide inhibitor. The Asn184 (PAP numbering) interacts with the inhibitor via a hydrogen bond.[17] In the psychrophilic structures, no interpretable $2F_0 - F_c$ electron density was present for all the residues in this flap.

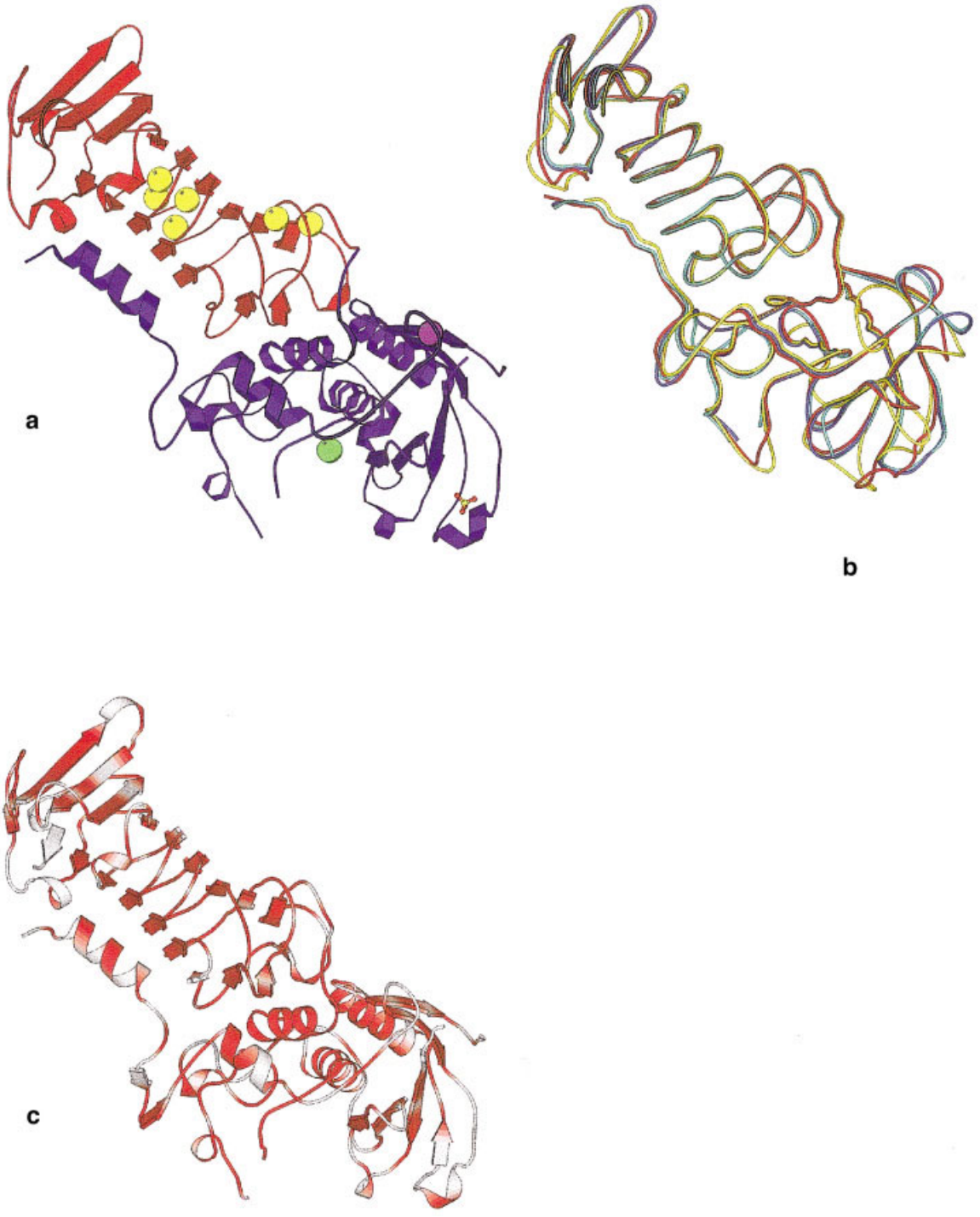

Fig. 2. (**a**) General overview of the structure of PAP. The N-terminal (catalytic) domain is blue and the C-terminal domain red. Calcium ions in the C-terminal domain are indicated as yellow spheres, the extra calcium in the N-terminal domain is purple, and the Zn ion green. A sulphate ion (only present in form 2) is shown in the catalytic domain as well. (**b**) Superposition of PAP form 1 (blue) and form 2 (cyan) with AP (red) and SMP (yellow). (a) and (b) were made using MOLSCRIPT.[45] (**c**) Representation of conserved regions coloured as degree of similarity with AP and serralysin (SMP), where red indicates highly conserved areas (drawing made using the program BOBSCRIPT[46]).

However, the small part of density observed for residues 182–183 clearly shows that the backbone follows the inhibitor-bound form of AP [Fig. 5(a)]. Further, an $2F_0 - F_c$ map calculated for form 1 partly shows the positions of residues 184 and 187, which also follow the main-chain of ligand-bound AP. In AP, the C_α atom of Asn191 (Asn184 in PAP) moves more than 12 Å upon inhibitor binding, whereas in SMP this movement is 3.6 Å.

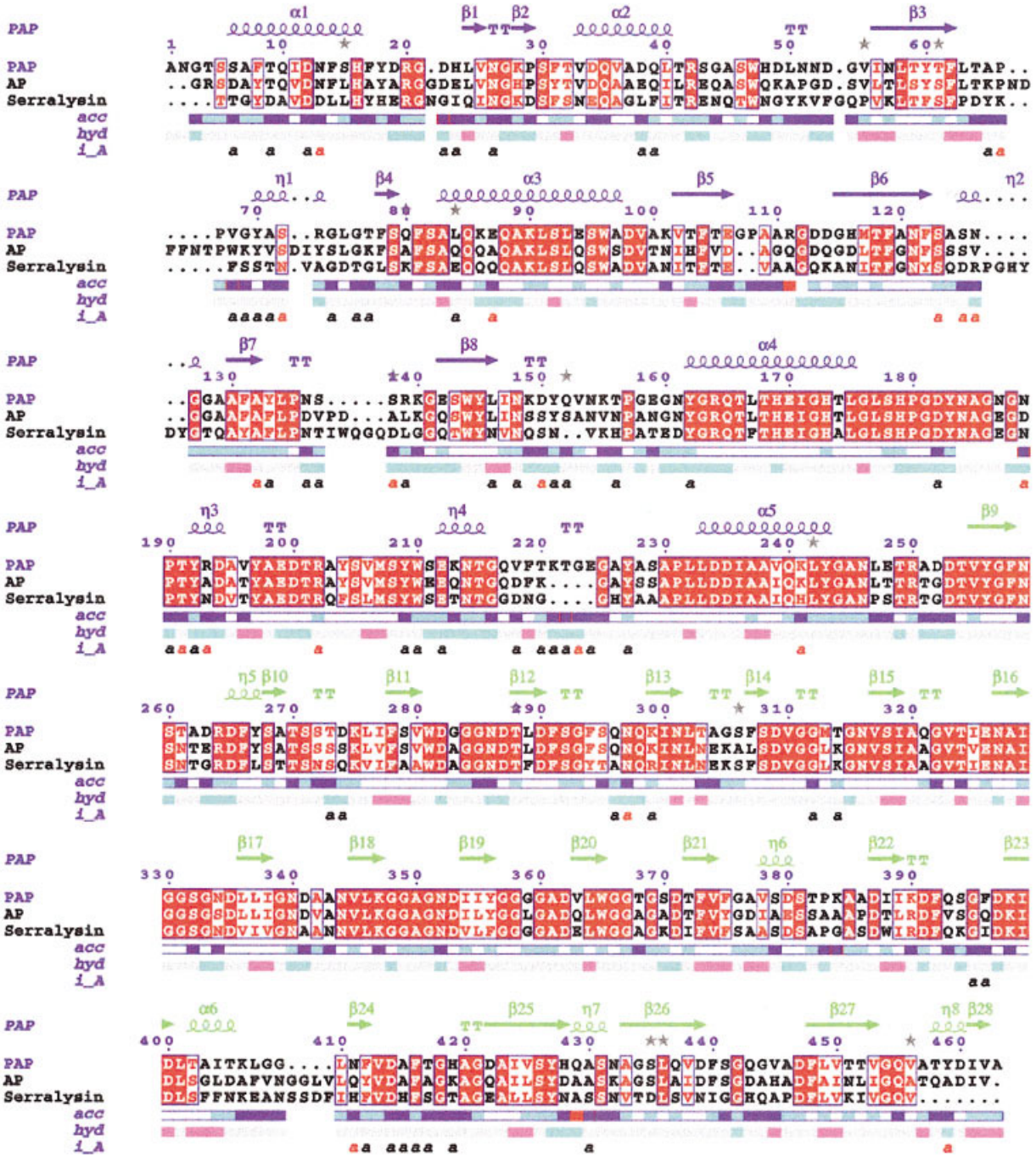

Fig. 3. Sequence alignment for PAP, AP, and SMP (serralysin). Secondary structure elements for PAP form 2 are indicated in blue for the catalytic domain and in green for the C-terminal domain. The accessibility of each residue from dark blue (accessible) to white (buried residues) as well as the hydropathic character of the sequence is shown, the latter varying from pink (hydrophobic parts) through grey (intermediate) and to cyan (hydrophilic parts). Crystal contacts less than 3.2 Å are indicated on the last line by a red "a" and between 3.2 and 4 Å by a black "a." Further, residues displaying double conformations in form 2 are marked with a grey star. The presentation of the sequence alignment[31] is made using ESPript.[47]

Other loop regions may also be important for accessibility to the active site. Compared to AP, an eight-residue deletion in loop 71–76 of PAP further provides a greater accessibility toward the active site [Fig. 5(b)]. However, this loop has the same length in PAP and SMP. In a fourth loop, comprising residues 137–139 in PAP, there is a four-residue deletion compared to SMP and a two-residue deletion compared to AP, also resulting in a more accessible active site in the psychrophilic enzyme.

A greater accessibility of the active site may result in a higher activity, but in contrast with this, site-directed mutagenesis experiments in a psychrophilic citrate syn-

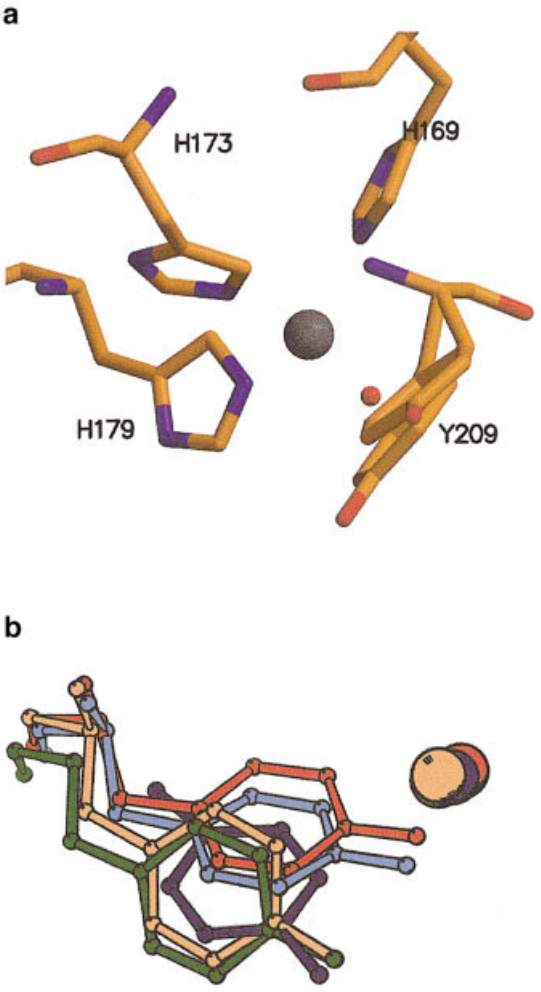

Fig. 4. (**a**) Zn^{2+} coordination site of PAP form 1 with the Zn^{2+} ion (grey sphere) coordinating three histidines (169, 173, and 179), a tyrosine (209), which has a double conformation, and a water molecule (red). (**b**) Superpositions of the active-site Tyr(209) and Zn^{2+} of PAP (the two conformations for crystal form 1 in blue and one conformation for form 2 in green with corresponding unligated (red) and ligated (light brown) Tyr in AP.

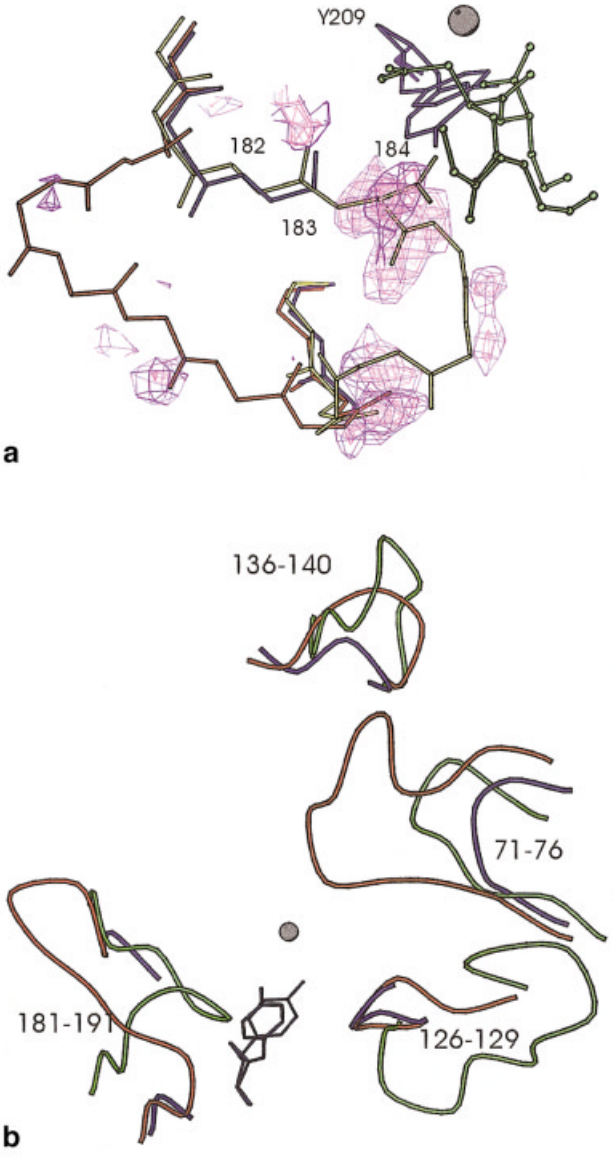

Fig. 5. (**a**) Superposition of the region near the active site; PAP form 1 (blue), free AP (red), and AP in complex with a tetrapeptide (yellow). This tetrapeptide is green. Tyr209 is in its double conformation and the central Zn^{2+} ion is shown as a grey sphere. Only the main-chain of the loop 182–190 (PAP numbering) is shown. The main-chain of residues 182 and 183 follows the main-chain of inhibitor-bound AP. An $F_0 - F_c$ map is shown for PAP, contoured at 2, 2.5, and 3.0σ. The nearby Asn184 (PAP numbering) that hydrogen bonds to the inhibitor in AP is highlighted (yellow). (**b**) Superposition of the four loops surrounding the active site in PAP (blue), AP (red), and SMP (green), all in their substrate-free conformation.Tyr209 of PAP is shown in its double conformation, and the central Zn^{2+} ion is shown as a grey sphere. Numbering is for the PAP residues. Both panels were made using MOLSCRIPT.[45]

thase did not compromise the enzyme's activity when the accessibility was reduced.[37]

Crystallographic Temperature Factors

Crystallographic B-factors, to a certain extent, reflect the flexibility of a protein structure. To compensate for differences due to crystal packing contacts, charged residues involved in intermolecular interactions are shown in Table II. The mean B-factor of every residue was divided by the mean B-factor of the whole protein, resulting in relative B-factors that indicate where the more flexible parts of the molecule are situated. Using relative B-factors, any bias due to systematically elevated B-factors caused by differences in temperature and quality of data collection, or in refinement procedure, is removed (Fig. 6).

Two stretches in PAP display high relative B-factors (up to 200%), which, in contrast, are low in the corresponding regions in the two mesophilic enzymes. The first stretch (residues 123–130) is one of the flaps that hinders the substrate entrance to the active site. The additional apparent flexibility observed in the PAP structure might therefore be partly responsible for the higher activity of this enzyme. The flexibility of the second stretch (residues 220-227) is also consistent with relatively high B-factors

TABLE II. Charged Residues Implicated in (A) Intermolecular and (B) Intramolecular Interactions[†]

PAP form 1	PAP form 2	AP	SMP
A			
Arg 139 NH2-Asn 52 O[a]	Lys 221 NZ-Asp 414 O[a]	Arg 2 NH1-Asp 256 OD1[a]	Glu 366 OE1-Lys 397 NZ[a]
Arg 139 NE-Asn 52 O[a]	Glu 87-Lys 241[a]	Arg 2 NH2-Thr 254 O[a]	Glu 366 OE2-Lys 397 NZ[a]
Arg 139 NE-Asp 53 O[a]		Asp 21 OD2-Arg 393[a]	
Arg 193 NH1-Ala 386 O[a]		Glu 42 OE1-Ser 156 OG[a]	
Lys 384 NZ-Gln 455 OE1[a]		Lys 84 NZ-Arg 41 O[a]	
Lys 398 NZ-Gly 21 O[a]		Asp 141 OD1-Asn 155[a]	
Arg 267 NH1-Gly 413 O[a]			
Arg 267 NH2-Gly 413 O[a]			
B			
Arg 20-Asp 234[b]	Arg 20-Asp 234[b]	Arg 18-Asp 237[b]	Arg 18-Asp 237[b]
Arg 164-Asp 265[b]	Arg 164-Asp 265[b]	Arg 171-Asp 268[b]	Arg 171-Asp 268[b]
Arg 250-Asp 98[b]	Arg 250-Asp 98[b]	Arg 253-Asp 105[b]	Arg 253-Asp 98[b]
Arg 264-Asp 98[b]	Arg 264-Asp 98[b]	Arg 267-Asp 105[b]	Arg 267-Asp 98[b]
Lys 90-Glu 106[b]	Lys 90-Glu 106[b]	Lys 97-Asp 113[b]	Lys 90-Glu 106[b]
Arg 42-Asp 182	Arg 42-Asp 182	Lys 74-Asp 67	Arg 41-Asp 189
Arg 73-Glu 142	Arg 73-Glu 142	Lys 227-Asp 225	Arg 302-Asp 312
Arg 264-Glu 94	Arg 264-Glu 94	Lys 244-Asp 33	Arg 393-Glu 366
Lys 275-Glu 224	Lys 275-Glu 224	Lys 244-Glu 37	Lys 308-Glu 33
	Lys 241-Asp 38	Lys 317-Asp 225	Lys 458-Asp 442
	Lys 221-Glu 224		

[†]For charge–charge interactions, a cutoff distance of 4.0 Å has been used. For hydrogen bonds between a charged residue and a noncharged side-chain, the cutoff was 3.5 Å.
[a]Residues belong to a symmetry-related molecule.
[b]Ionic interactions conserved between PAP, AP, and SMP.

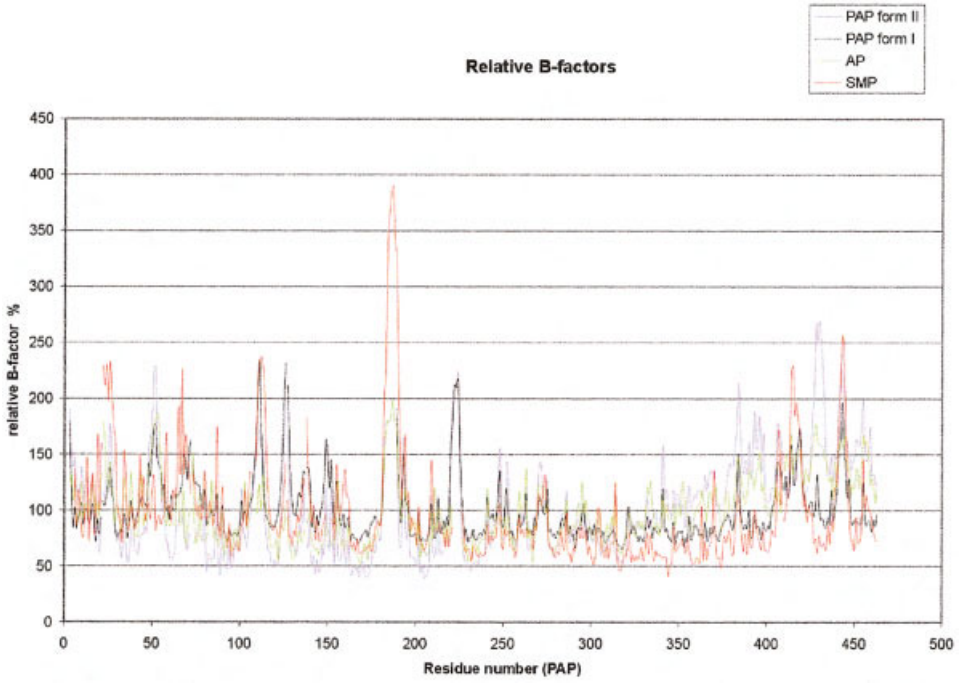

Fig. 6. Relative B-factors for PAP forms 1 and 2, AP, and SMP (%). The residue numbering corresponds to PAP [Fig. 2(a)]. Gaps in the curves correspond to deletions or residues with missing electron density.

and can be partly explained by a four-residue insertion in the psychrophilic sequence, situated at the interface between the two domains but pointing toward the solvent and far away from the active site. We suggest that deletion of these four residues by site-directed mutagenesis may provide an improved thermostability to the enzyme.

One of the regions with high B-factors in PAP, AP, and SMP is the loop comprising residues 182–189 (PAP numbering), which displays a different conformation in AP and SMP upon substrate binding. Relative B-factors extend up to 390% in SMP and to 189% in AP. Although this loop was not entirely modeled in PAP, the relative B-factors for

residues 182 and 183 lie between those for the corresponding residues in AP and SMP, with values up to 147% (form 1), 180% (form 2), 163% (AP), and 214 % (SMP).

Ionic Pairs and Hydrogen Bonds

The number of intramolecular hydrogen bonds in the various crystal structures differs only marginally, with 410 (form 1) and 429 (form 2) for PAP and 411 for both AP and SMP. The psychrophilic structures display 9 (form 1) or 11 (form 2) salt bridges, while this number is 10 for both mesophilic enzymes (Table II). Five of these intramolecular ionic pairs are conserved among the four structures. Care must be taken when interpreting these numbers because they can vary due to differences in crystal contacts as reflected in the number of intramolecular H bonds in forms 1 and 2. In the SMP structure, the side-chains of only two charged residues are implicated in crystal contacts, while in AP eight different charged side-chains are involved in such contacts.

In the case of other cold-adapted enzymes, it has been observed that the total number of salt bridges is equal to, or even higher than, that found in known mesophilic or thermophilic counterparts.[5,7,8] The number of interdomain salt bridges, however, is lower in the psychrophilic proteins, indicating the relative importance of such ionic interactions at higher temperatures. Proteins may be denatured not only by heat but also by cold.[38] Additional protection against low-temperature denaturation can be acquired by the formation of extra ionic pairs, which may also explain why the number of salt bridges in the 3D structures of PAP and AP is almost invariant.

Accessible Surface Areas and Hydrophobicity

PAP has a total accessible surface area of 18510 Å^2 (form 1) and 18718 Å^2 (form 2) compared to 19076 Å^2 for AP and 18987 Å^2 for SMP. The accessible areas for hydrophobic residues comprise 24.0, 23.6, 24.3, and 22.4% of the total surface, respectively, showing that the differences between the three enzymes are small. In contrast, an increased exposure of hydrophobic residues has been reported for other cold-adapted enzymes.[5,7,39,40] About 20% of the residues F, I, L, and V involved in the stabilization of AP appear to be mutated in PAP,[15] leading to a significant decrease of the overall hydrophobicity. It was also found that the aliphatic index[41] and the grand average of hydropathicity[42] are lower for PAP than for AP.

The packing of hydrophobic side-chains in protein cores leads to a large gain in entropy due to the release of water molecules solvating them, resulting in a net stabilization of most proteins. At low temperatures, this entropy gain is reduced, probably because of the loss of mobility of the released water molecules, which may explain why there is little difference in the exposure of hydrophobic residues.

Loop Lengths, Glycines, Prolines, and Arginines

Structural alignment shows that PAP has a four-residue insertion and a four-residue deletion compared to AP and SMP. When compared to AP alone, PAP has an extra eight-residue deletion. Relative to SMP, however, there is an insertion of six residues and two deletions of five residues. Overall, and in contrast to other cold-adapted enzymes,[4,5,43] PAP has more deletions than insertions compared to the mesophilic counterparts.

Regarding amino acid residues that may confer flexibility, rigidity, or stability to a 3D structure, the number of glycines (flexibility) is only slightly increased, with 60 for PAP, 55 for AP, and 58 for SMP. For PAP, 55 of these occur in loop regions, while this number is 50 for AP and 52 for SMP. There are 10 prolines (rigidity) in PAP, 11 in AP, and 10 in SMP, all occurring in loop regions. In PAP there are 10 arginines (stability), compared to 9 and 8 for AP and SMP, respectively, showing that there is no significant decrease in arginine content in PAP, in contrast to the situation in other cold-adapted proteins.[5,7]

Calcium Binding Sites

Besides the Zn^{2+} in the active site, PAP binds eight calcium ions in crystal form 1 and seven in crystal form 2. In both forms, one calcium ion is bound at the same site in the proteolytic domain, the remaining ones being bound in the C-terminal domain. In the structures of AP and SMP, eight and seven calcium ions are present, respectively, but they are all bound in the C-terminal domain. The seven calcium ions that appear in SMP are strictly conserved in AP and PAP form 1, but not in PAP crystal form 2 where one calcium ion, Ca 501 (form 1), is replaced by a water molecule (Wat154). This could be a consequence of differences in the EDTA concentration used during enzyme preparation. The latter calcium site is the most accessible

TABLE III(A). Relative B-Factors for Calcium Ions[†]

PAP			
Form 1	Form 2	AP	SMP
(500/700) 128%	159%		
(501/water) 82%	—	(505) 125%	(478) 74%
(502/704) 78%	103%	(504) 107%	(477) 67%
(503/703) 81%	86%	(503) 80%	(475) 66%
(504/706) 86%	101%	(507) 91%	(479) 67%
(505/705) 85%	98%	(506) 102%	(476) 53%
(506/702) 83%	97%	(502) 90%	(474) 62%
(507/701) 88%	83%	(501) 89%	(473) 71%
		(508) 226%	

[†]The B-factor for each calcium was divided by the mean B-factor of the protein structure to which it belongs. Calcium ions from the respective structures that are spatially equivalent are presented on the same line. The calcium numbering is given in brackets.

TABLE III(B). Distances Between the Ca^{2+} in the Catalytic Domain of PAP and Ligated Residues

Distances in (Å) between Ca (500/700) and	Crystal form 1	Crystal form 2
Asp49 OD2 form 1/OD1 form 2	2.54	2.29
Asp114 OD2	2.54	2.32
Val55 O	2.47	2.30
Asp53 OD1 form 1/OD2 form 2	2.59	2.38
Asn57 ND2 form 1/OD1 form 2	2.59	2.28
Asn51 OD1	3.98	2.39

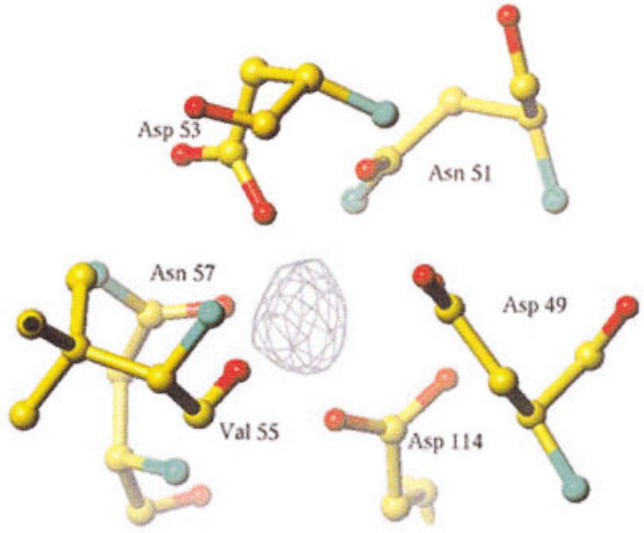

Fig. 7. Anomalous difference Fourier map contoured at 4σ showing the novel calcium ion in the N-terminal domain of PAP, form 2, surrounded by the ligating amino acid residues Asp49, Asn51, Asp53, Val55, Asn57 and Asp114.

one, consistent with its relatively high thermal B-factor [Table III(a)].

For the extra calcium ion in the catalytic domain in both crystal forms of PAP (Fig. 7), distances to its ligands are given in Table III(b). It appears that this ion is weakly bound, especially in form 1. Although the calcium site is situated in a region easily accessible to the solvent, no electron density for water molecules was found in its immediate vicinity. Binding of this calcium induces a 13-Å movement in C_α positions of a loop (residues 107–116) compared to the mesophilic enzymes. Asp114 is a Ca ligand in this loop and is replaced by a Gln in AP and Lys in SMP, which both are less efficient chelating agents. Asp49, another ligand, is substituted by Lys in AP and by Gly in SMP. The extended chain length due to a two-residue insertion of Gly and Pro at the beginning of the displaced loop in PAP may facilitate the drastic loop movement. The mean relative B-factors for this loop are 144.4% (PAP form 1), 126.2% (PAP form 2), 108.9% (AP), and 164.0% (SMP), demonstrating that its relative flexibility in PAP is between that in AP and SMP.

PAP displays a greater sensitivity toward moderate EDTA concentrations.[15] The weak chelation of the calcium ion in the proteolytic domain and its close proximity to the solvent partly explain this sensitivity, which is also supported by a relatively higher B-factor [Table III(a)] compared to the other calcium ions.

In the mesophilic AP structure, there is an extra calcium site (calcium 508) that has been interpreted as being partially occupied.[16] Its ligands are structurally conserved in PAP, except for Asp443 (PAP numbering) being replaced by Gln in PAP, which is a less efficient chelator for Ca^{2+} and explains the absence of a calcium ion in this region of the psychrophilic enzyme. In SMP, this binding is not conserved, as a proline residue is distorting the whole site.

The loss of the latter calcium in PAP may be partially responsible for the thermolability of the psychrophilic enzyme but is not an exclusive psychrophilic trait as there is no calcium site in SMP either. Mutating Gln443 to Asp might help in creating a ninth calcium binding site in PAP, thereby increasing the thermostability. This expected improvement of enzyme stability would probably not interfere with the low-temperature activity because the engineered calcium site would be located far from the active site in the noncatalytic domain. In addition, the loss of one calcium in crystal form 2, indicative of a reduced stability, also suggests that mutating Phe396 to Gln near this calcium site may help in stabilizing the overall structure and increasing its resistance toward EDTA.

CONCLUSION

Psychrophilic enzymes are characterized by their higher activity at low and moderate temperatures when compared to their mesophilic counterparts and, therefore, have attracted increasing attention in recent years owing to their biotechnological potential.[1,44]

The most striking feature of the PAP structures compared to its mesophilic homologs is the 13-Å conformational change triggered by a calcium ion in the proteolytic domain, together with a higher degree of accessibility of the active site. This change is not related to crystal packing effects because it is observed in both crystal forms obtained under different crystallization conditions.

The crystal structures of PAP thus indicate a region of high conformational flexibility that is proposed to be important for regulating both substrate access and product release. The active site of the psychrophilic alkaline protease being more open and flexible is shown to correspond rather to the substrate-bound forms of AP and SMP than to the substrate-free mesophilic enzymes. These structures therefore provide additional support for the hypothesis that psychrophilic enzymes achieve efficient catalysis by increased flexibility, at least of the active-site region, and thereby suggest that PAP can easily accommodate substrates at low energy costs with its active site being more accessible than those of the mesophilic counterparts.

Compared to AP, but not to SMP, one calcium ion has been lost in one of the crystal forms of PAP (form 2), which can be considered as a destabilizing factor. Besides this loss, none of the other characteristics—such as ionic pairs, hydrogen bonds, surface hydrophobicity, loop regions, proline content, and glycine and arginine distribution—can explain a decreased stability of the psychrophilic enzyme. However, the local flexibility observed in and around the active site of PAP, combined with its higher accessibility, can be determinants for efficient catalysis at low temperature. This suggests the possibility of designing an enzyme being active at low temperatures but stable at moderate temperatures. A possible strategy for stabilization of PAP would be using site-directed mutagenesis to rearrange the accessible calcium site and introduce a new one that already exists in a mesophilic homologue, both far from the active site. Such experiments are on the way.

ACKNOWLEDGMENTS

The authors thank the Institut Français pour la Recherche et la Technologie polaire for the generous accommodation of our research fellows at the Antarctic station J.S. Dumont-d'Urville. N.A. was supported by the EU COLDZYME program. F.V.P. is a research fellow of the Fund for Scientific Research-Flanders. The authors thank P. Gouet for help with the ESPript representation.

REFERENCES

1. Russell NJ. Molecular adaptations in psychrophilic bacteria: potential for biotechnological applications. Adv Biochem Eng Biotech 1998;61:1–21.
2. Feller G, Gerday C. Psychrophilic enzymes: molecular basis of cold adaptation. Cell Mol Life Sci 1997;53:830–841.
3. Gerday C, Aittaleb M, Arpigny JL, Blaise E, Chessa J-P, Garsoux G, Petrescu I, Feller G. Psychrophilic enzymes: a thermodynamic challenge. Biochim Biophys Acta 1997;1342:119–131.
4. Feller G, Narinx E, Arpigny JL, Aittaleb M, Baise E, Genicots S., Gerday C. Enzymes from psychrophilic organisms. FEMS Microbiol Rev 1996;18:189–202.
5. Aghajari N, Feller G, Gerday C, Haser R. Structures of the psychrophilic *Alteromonos haloplanctis* α-amylase give insights into cold adaptation at a molecular level. Structure 1998;6:1503–1516.
6. Aghajari N, Feller G, Gerday C, Haser R. Crystal structures of the psychrophilic α-amylase from *Alteromonas haloplanctis* in its native form and complexed with an inhibitor. Protein Sci 1998;7:564–572.
7. Russell RJ, Gerike U, Danson MJ, Hough DW, Taylor GL. Structural adaptations of the cold-active citrate synthase from an Antarctic bacterium. Structure 1998;6:351–361.
8. Kim S-Y, Hwang KY, Kim S-H, Sung H-C, Han YS, Cho Y. Structural basis for cold adaptation. Sequence, biochemical properties, and crystal structure of malate dehydrogenase from a psychrophile *Aquaspirillium arcticum*. J Biol Chem 1999;274:11761–11767.
9. Alvarez M, Zeelen JP, Mainfroid V, Rentier-Delrue F, Martial JA, Wyns L, Wierenga RK, Maes D. Triose-phosphate isomerase (TIM) of the psychrophilic bacterium *Vibrio marinus.* Kinetic and structural properties. J Biol Chem 1998;273:2199–2206.
10. Feller G, Payan F, Theys F, Qian M, Haser R, Gerday C. Stability and structure analysis of α-amylase from the Antarctic psychrophile *Alteromonas haloplanctis* A23. Eur J Biochem 1994;222:441–447.
11. Arpigny JL, Lamotte J, Gerday C. Molecular adaptation to cold of an Antarctic bacterial lipase. J Mol Catal B 1997;3:29–35.
12. Narinx E, Baise E, Gerday C. Subtilisin from psychrophilic Antarctic bacteria: characterization and site-directed mutagenesis of residues possibly involved in the adaptation to cold. Protein Eng 1997;10:101–109.
13. Petrescu I, Lamotte-Brasseur J, Chessa J-P, Ntarima P, Claeyssens M, Devreese B, Marino G, Gerday C. Xylanase from the psychrophilic yeast *Cryptococcus adeliae*. Extremophiles 2000;4:137–144.
14. Bentahir M, Feller G, Aittaleb M, Lamotte-Brasseur J, Himri T, Chessa J-P, Gerday C. Structural, kinetic and calorimetric characterization of the cold-active phosphoglycerate kinase from the Antarctic *Pseudomonas* sp. TAC II 18. J Biol Chem 2000;275:11147–11153.
15. Chessa J-P, Petrescu I, Bentahir M, Van Beeumen J, Gerday C. Purification, physico-chemical characterization and sequence of a heat labile alkaline metalloprotease isolated from a psychrophilic *Pseudomonas* species. Biochim Biophys Acta 2000;36103:1–10.
16. Baumann U, Wu S, Flaherty KM, McKay DB. Three-dimensional structure of the alkaline protease of *Pseudomonas aeruginosa*: a two-domain protein with a calcium binding parallel beta roll motif. EMBO J 1993;12:3357–3364.
17. Miyatake H, Hata Y, Fujii T, Hamada K, Morihara K, Katsube Y. Crystal structure of the unliganded alkaline protease from *Pseudomonas aeruginosa* IFO3080 and its conformational changes on ligand binding. J Biochem 1995;118:474–479.
18. Baumann U. Crystal structure of the 50 kDa metallo protease from *Serratia marcescens*. J Mol Biol 1994;242:244–251.
19. Baumann U, Bauer M, Létoffé S, Delepelaire P, Wandersman C. Crystal structure of a complex between *Serratia marcescens* metallo-protease and an inhibitor from *Erwinia chrysanthemi*. J Mol Biol 1995;248:653–661.
20. Hamada K, Hata Y, Katsuya Y, Hiramatsu H, Fujiwara T, Katsube Y. Crystal structure of *Serratia* protease, a zinc-dependent proteinase from *Serratia* sp. E-15, containing a β-sheet coil motif at 2.0 Å resolution. J Biochem 1996;119:844–851.
21. Lakowicz JR, Weber G. Quenching of protein fluorescence by oxygen. Detection of structural fluctuations in proteins on the nanosecond time scale. Biochemistry 1973;12:4171–4179.
22. Lakowicz JR. Principles of fluorescence spectroscopy. New York: Plenum Press; 1983.
23. Villeret V, Chessa J-P, Gerday C, Van Beeumen J. Preliminary crystal structure determination of the alkaline protease from the Antarctic psychrophile *Pseudomonas aeruginosa*. Protein Sci 1997;6:2462–2464.
24. Aghajari N. PhD thesis. Université de la Méditerranée Aix-Marseille II & Université de Liège; 1998.
25. Navaza J. AMoRe: an Automated Package for Molecular Replacement. Acta Crystallogr 1994;A50:157–163.
26. The CCP4 Suite: Programs for protein crystallography. Acta Crystallogr 1994;D50:760–763.
27. Read RJ. Improved Fourier coefficients for maps using phase from partial structure with errors. Acta Crystallogr 1986;A42:140–149.
28. Roussel A, Cambillau C. In: Silicon Graphics geometry directory 86. Mountain View, CA: Silicon Graphics; 1991.
29. Brünger AT, Adams PD, Clore GM, DeLano WL, Gros P, Grosse-Kunstleve RW, Jiang JS, Kuszewski J, Nilges M, Pannu NS, Read RJ, Rice LM, Simonson T, Warren GL. Crystallography and NMR system: A new software suite for macromolecular structure determination. Acta Crystallogr 1998;D54:905–921.
30. Laskowski RA, MacArthur MW, Moss DS, Thornton JM. PROCHECK: a program to check the stereochemistry of protein structures. J Appl Crystallogr 1993;26:283–291.
31. Thompson JD, Higgins DG, Gibson TJ. CLUSTAL W: improving the sensitivity of progressive multiple sequence alignment through sequence weighting, position-specific gap penalties and weight matrix choice. Nucleic Acids Res 1994;22:4673–4680.
32. Kabsch W, Sander C. Dictionary of protein secondary structure: pattern recognition of hydrogen-bonded and geometrical features. Biopolymers 1983;22:2577–2637.
33. McDonald IK, Thornton JM. Satisfying hydrogen-bonding potential in proteins. J Mol Biol 1994;238:777–793.
34. Nicholls A, Sharp KA, Honig B. Protein folding and association: insights from the interfacial and thermodynamic properties of hydrocarbons. Proteins 1991;11:281–296.
35. Bode W, Gomis-Rüth FX, Stöcker W. Astacins, serralysins, snake venom and matrix metalloproteinases exhibit identical zinc-binding environments (HEXXHXXGXXH and Met-turn) and topologies and should be grouped into a common family, the "metzincins." FEBS Lett 1993;331:134–140.
36. Lovell SC, Word JM, Richardson JS, Richardson DC. The penultimate rotamer library. Proteins 2000;40:389–408.
37. Gerike U, Danson MJ, Hough DW. Cold-active citrate synthase: mutagenesis of active-site residues. Protein Eng 2001;14:655–661.
38. Graziano G, Catanzano F, Riccio A, Barone GJ. A reassessment of the molecular origin of cold denaturation. Biochem 1997;122:395–401.
39. Smalås AO, Heimstad ES, Hordvik A, Willasen P, Male R. Cold adaptation of enzymes: structural comparison between salmon and bovine trypsins. Proteins 1994;20:149–166.
40. Wallon G, Lovett ST, Magyar C, Svingor A, Szilagvi A, Zadovsky P, Ringe D, Petsko GA. Sequence and homology model of 3-ispopropylmalate dehydrogenase from the psychrotrophic bacterium *Vibrio* sp I5 suggest reasons for thermal instability. Protein Eng 1997;10:665–672.
41. Ikai A. Thermostability and alphatic index of globular proteins. J Biochem 1980;88:1895–1898.

42. Kyte J, Doolittle RF. A simple method for displaying the hydropathic character of a protein. J Mol Biol 1982;157:105–132.
43. Davail S, Feller G, Narinx E, Gerday C. Cold adaptation of proteins. Purification, characterization, and sequence of the heat-labile subtilisin from the antarctic psychrophile *Bacillus* TA41. J Biol Chem 1994;269:17448–17453.
44. Gerday C, Aittaleb M, Bentahir M, Chessa J-P, Claverie P, Collins P, D'Amico S, Dumont J, Garsano G, Georlette D, Hoyoux A, Lonhienne T, Meuwis M-A, Feller G. Cold-adapted enzymes: from fundamentals to biotechnology. Trends Biotech 2000;18:103–107.
45. Kraulis PJ. MOLSCRIPT: a program to produce both detailed and schematic plots of protein structures. J Appl Crystallogr 1991;24:946–950.
46. Esnouf RM. An extensively modified version of MOLSCRIPT that includes greatly enhanced coloring capabilities. J Mol Graph 1997;15:132–134.
47. Gouet P, Courcelle E, Stuart DI, Metoz F. ESPript: multiple sequence alignments in PostScript. Bioinformatics 1999;15:305–308.